Al-Sibd Center for Research and Scholarly Publishing
Journal of Energy Sustainability and Economics (JESE)
Journal Homepage : https://jese.srp-center.iq/

Numerical study on improving the thermal performance of an electric motor of an oil pump using an earth air heat exchanger (EAHE).

Baraa A. Gaber[1] , Rafid M. Hannun[2]

[1,2] College of Mechanical Engineering, University of Thi-Qar, Iraq

Corresponding Author : Baraa.a.s@utq.edu.iq

Keywords:

Cooling; Electric Engine; EAHE; Thermal Performance; CFD Modelling;

Abstract

High temperatures in electric motors are a major cause of reduced efficiency and shortened lifespan. To mitigate this problem, an earth air heat exchanger can be used as an effective cooling system. This research investigates improving the thermal performance of electric motors by analyzing the effect of pipe length. Five pipe lengths (10 m, 30 m, 50 m, 70 m, and 90 m) and three inlet temperatures (30°C, 40 °C, and 50 °C) were selected, with a constant mass flow rate of 0.6 kg/s and a constant diameter of 6 in, to determine cooling efficiency. The results showed that rising tube length led to a significant improvement in cooling, with the heat exchanger exit temperature decreasing more at longer lengths. This is attributed to the larger surface area for heat transfer. Larger lengths are associated with higher pressure differentials and greater pumping capacity. Despite this, the longest length performed best, achieving the highest cooling efficiency, with a reduction in motor temperature of approximately 4.75%, 7. 33%, 8. 28%, 8.60%, and 11.21% for pipe lengths of 10 m, 30 m, 50 m, 70 m, and 90 m, respectively. This means that the greater the length, the greater the drop in temperature, resulting in higher system efficiency.

.

Introduction

The earth air heat exchanger is one of the most important components that improves electric motor performance and efficiency. Therefore, using an earth air heat exchanger (EAHE) for cooling is beneficial for increasing cooling efficiency, extending its lifespan, and preventing malfunctions by burying the EAHEs in the soil. Benhamou and Draoui [1] investigated the performance of EAHEs utilized to cool buildings in the Algerian Sahara during the summer. The researchers employed a 1D transient model to analyze the impact of dynamic and geometric parameters on the thermal performance of EAHEs. The soil temperature was 22.271°C, and the EAHE tube had a thickness of 5 mm. They discovered that the exhaust air temperature rises with rising tube cross-section and air velocity, but decreases with increasing tube length. Hannun et al. [2]

explored the cooling of a 250 kVA transformer using an air-ground heat exchanger in Nasiriyah. The maximum temperature reached 50°C. Their results showed that the transformer temperature decreased with rising tube length and burial depth. They observed that rising air velocity reduced the transformer temperature. The heat exchanger resulted in a temperature reduction of 18.5%. Hasan and Sajad [3] conducted a numerical

analysis on the impact of multiple design parameters (outlet condition, boundary condition at the intake, tube diameter, and tube length) on the performance of an EAHE with four diameters. The pipes were underground, embedded three meters deep and fifty meters long. The results showed that the 6-inch diameter had the best overall performance, but the 2-inch diameter performed better in terms of thermal performance. Masselli and Greco [4] assessed the effect of the performance of a horizontal single-channel EAHE in the city of Naples. Their study proved that the thermal performance rises as the length increases, and that a smaller diameter improves the cooling process because the air is brought up to a temperature close to the earth's temperature. It was found that the optimal configuration is at a 50 m length, a 0.1m diameter, and a speed of 1.5 meter per second. Hasan and Muter [5] evaluated the impact of design specifications for an EAHE used in Nasiriyah to cool poultry houses. They studied several lengths (355m, 370m, 385m, 395m, and 410m) with pipe diameters of 2, 3, 4, and 6 inches at a constant mass flow rate of 22948.2 kg/s. The outcomes demonstrated that the heat emitted from the exchanger decreased with rising ambient temperature, increased with increasing brick thickness, and decreased with rising diameter. The longest length, 410m, provided the best thermal performance. Ahmed and Prakash [6] experimented with an EAHE utilized as a heating apparatus in India. They used three horizontal PVC tubes of different diameters. Their findings revealed that smaller tubes at low speeds produced the greatest increase in output temperature, with an efficiency of 0.83 at 2 m/s. As the speed increased, the heat exchange and performance of the EAHE decreased. Albarghouth et al.[7] assessed a numerical and empirical investigation on several parameters on the performance of an EAHE for building cooling in Karbala. The results illustrated that the percentage decrease was 28.3%, 25.5%, and 19.5% at inlet temperatures of 41°C, 45°C, and 49.5°C, respectively. Increasing the pipe length decreased the exit temperature from the heat exchanger and increased the heat transfer rate, as observed at a length of 62.1 m, where the temperature of 26°C. Diedrich et al. [8] evaluated a computational model for analyzing the performance of an EAHE utilizing an ANSYS/Fluent program. This system relied on a constant soil temperature. The researchers tested two simplified models to speed up calculations, including assuming a constant surface temperature of 23.7°C on the heat exchanger tube at a 1.5-meter depth, and a decrease in soil zone extending 0.5 meters in all directions for the zigzag heat exchanger. Their results showed that the two models were very close to the real data. Hasan and Hummood [9] conducted an empirical investigation using an air-ground heat exchanger for air supply compressor cooling. They used a pipe that was 11.88 meters long, 2 inches in diameter, and 3.5 meters deep. Their findings showed that, despite the high entrance temperature, the exit temperature remained low due to the consistent ground temperature, ensuring effective cooling. Nasr et al.[10] presented a modern cooling technology to improve the efficiency of the electric generator using an air-ground heat exchanger. Using MATLAB for simulation, their findings indicated that the temperature exiting the heat exchanger reduces with rising tube length. They noted a 24.45% decrease in the generator's temperature when operating at full power, and a further 50.91% decrease when the load increased, due to the EAHE.

Although many previous studies have addressed the use of an EAHE in various cooling applications, no studies have specifically focused on the cooling of electric motors. Therefore, this research aims to study the thermal performance of an EAHE used to cool an electric oil pump motor under the arid climatic conditions of Nasiriyah. This is achieved using numerical simulation. The research also focuses on analyzing the effect of length, inlet air temperature, constant air mass flow rate, and pipe diameter on reducing motor temperature and improving cooling efficiency.

Problem Description

Among the factors that pose the greatest consideration for the efficiency and service life of the electric motors are high temperatures in the motors. The temperature that develops in the electric motor causes more copper loss and greater resistance of the winding, thus less efficiency and a shorter lifespan. The present research paper explores ways of enhancing the efficiency of electric motors by increasing the efficiency of motor cooling with an air-earth heat exchanger.

The model used in this research is a three-phase squirrel-cage induction motor (TEFC), as demonstrated in Figure 1. In this model, the motor's external fins, which are 750 mm long and 550 mm in diameter, were used to reduce the complexity of the model, as shown in Figure 2.

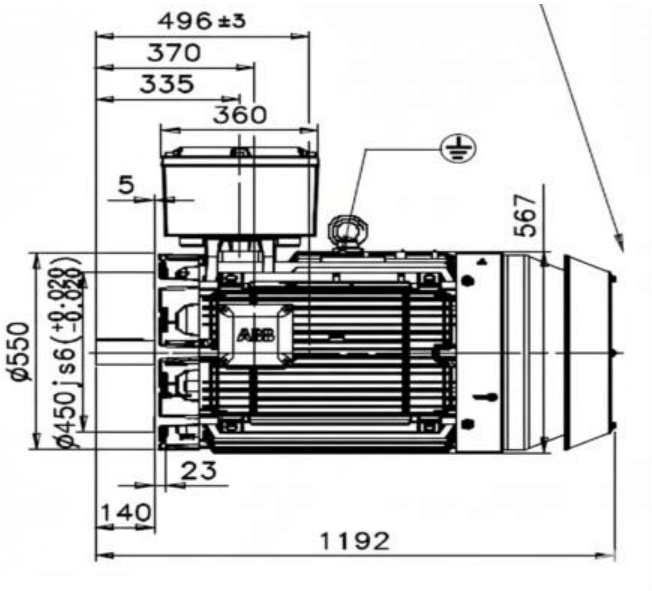

Figure 1: The schematic diagram of an electric motor(130A).

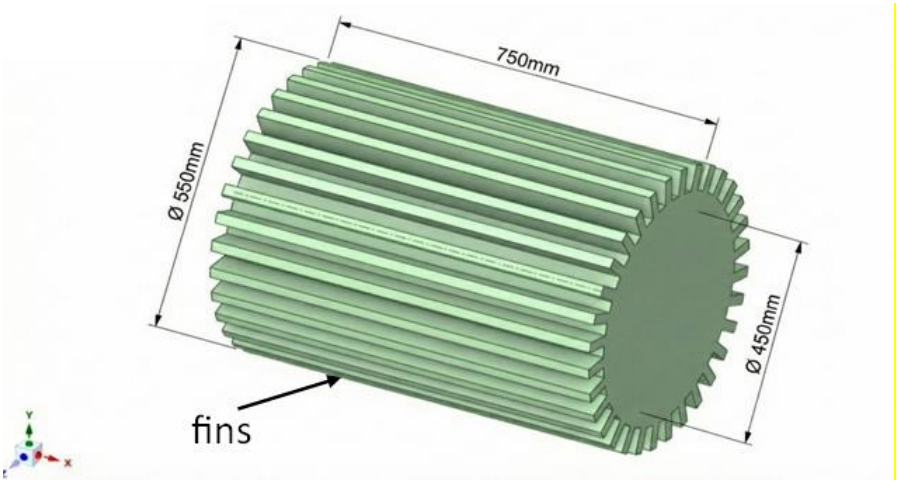

Figure 2: Geometry of the electric motor.

The electric motor was cooled using an earth-air heat exchanger. It was buried underground with internal pipes (6 in) in diameter and lengths of 10 m, 30 m, 50 m, 70 m, and 90 m, at a constant mass flow rate of 0.6 kg/s. The proposed design is illustrated in Figure 3. Polyvinyl chloride (PVC) was chosen for this study.

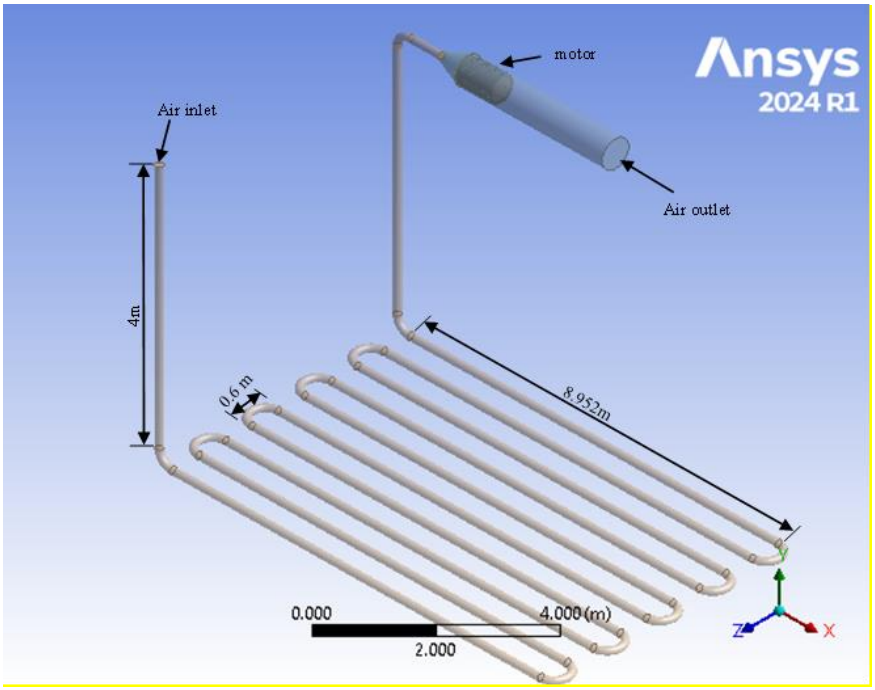

Figure 3: Modeling the geometry of the EAHE.

Disturbed Soil

Heat transmission damaged the soil layer near the surface of the EAHE tubes, resulting in thermally disturbed soil, as illustrated in Figure 4. There was no defined rule for determining the disturbed soil thickness. According to numerous investigations, the thickness of the disturbed soil equals the diameter of the tube [11], four times the diameter of the tube [12], twice the diameter of the tube [13], and ten times the diameter of the tube [14]. Studies have also demonstrated that operating geothermal heat exchange systems in both winter and summer reduces the impact of disturbed soil on their performance [15]. This study assumes that the disturbed soil thickness is equal to double the tube diameter, as in [16].

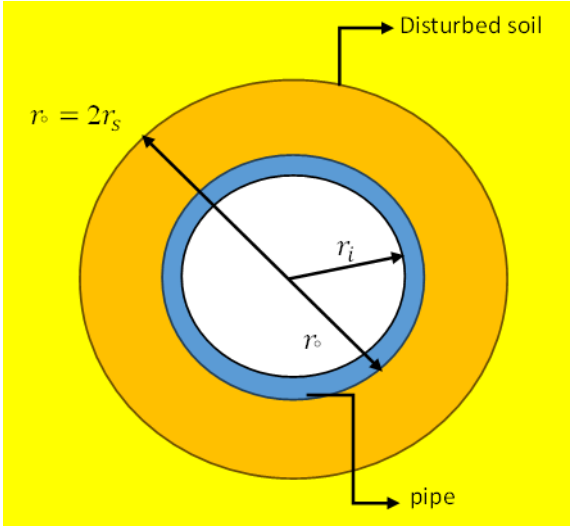

Figure 4: The cross-section of the EAHE tube.

The air's physical properties, including heat, soil, and tube material (PVC), were presumed to be constant. Table 1 below shows their values [3, 5,17].

Table 1: Thermal and physical parameters of the material.

Material	Density (kg/m^3)	Specific heat (J/kg ˚C)	Thermal conductivity (W/m ˚C)
Air	1.225	1006.5	0.0242
Saturated soil	2000	880	1.4
PVC	1380	900	0.16

Mathematical Model

Governing Equations

The following equations are used in this study for heat transfer and fluid flow [9]:

A.1 Continuity Equation:

(1)

$$\text{div}\,\overline{V} = 0$$

A.2 Momentum Equation:

X - direction

$$\text{div}\left(\overline{u}\,\overline{V}\right) + \text{div}\left(\overline{u'V'}\right) = -\frac{1}{\rho}\frac{\partial \overline{p}}{\partial \overline{x}} + \nu\,\text{div}\left(\text{grad}\left(\overline{u}\right)\right) \quad (2)$$

Y - direction

$$\text{div}\left(\overline{v}\,\overline{V}\right) + \text{div}\left(\overline{v'V'}\right) = -\frac{1}{\rho}\frac{\partial \overline{p}}{\partial \overline{y}} + \nu\,\text{div}\left(\text{grad}\left(\overline{v}\right)\right) \quad (3)$$

Z - direction

$$\text{div}\left(\overline{w}\,\overline{V}\right) + \text{div}\left(\overline{w'V'}\right) = -\frac{1}{\rho}\frac{\partial \overline{p}}{\partial \overline{w}} + \nu\,\text{div}\left(\text{grad}\left(\overline{w}\right)\right) \quad (4)$$

A.3 Energy Equation:

$$\frac{\partial U\widetilde{T}}{\partial x} + \frac{\partial V\widetilde{T}}{\partial y} + \frac{\partial w\widetilde{T}}{\partial z} = \frac{k}{\rho\,cp}\left(\frac{\partial}{\partial x}\left(\frac{\partial \widetilde{T}}{\partial x}\right) + \frac{\partial}{\partial y}\left(\frac{\partial \widetilde{T}}{\partial y}\right) + \frac{\partial}{\partial z}\left(\frac{\partial \widetilde{T}}{\partial z}\right)\right) \quad (5)$$

The coefficient of performance (COP) is utilized to evaluate the (EAHE) system [18].

$$COP = \frac{Q}{P.P} \quad (6)$$

$$Q = \dot{m}C_p\Delta T \quad (7)$$

$$P.P = \Delta P.V \quad (8)$$

$$\Delta P = P_{in} - P_{out} \quad (9)$$

The percentage of temperature reduction for an electric motor fitted with an (EAHE) system is calculated as follows:

Percentage Reduction= $\frac{\overline{T}-\overline{\overline{T}}}{\overline{T}} \times 100\%$ (10)

$\overline{T}$: The temperature before the cooling process.

$\overline{\overline{T}}$: The temperature after the cooling process.

Boundary Conditions

The temperature of the incoming dry bulb (Tin) is constant within the inner part of the EAHE tube and was utilized as a limit condition. The pressure at the outlet was measured to be equivalent to atmospheric pressure.

The horizontal cross-section of the EAHE tubes is equal to the thickness of the disturbed soil at the outer surface walls by a distance of 2 mm, where the soil temperature is constant at 26°C at a 4-meter depth.

Temperature of the soil

Predict soil temperature based on annual ambient temperature variation. Moreland et al. [19], Kosuda et al. [20], and Labes [21] presented a mathematical relationship. The soil temperature prediction reliability is closely related to the value of the input factors, as illustrated:

$$T_{(z,t)} = T_m - A_s e^{(-z(\pi/8760\alpha)^{0.5})} \times \cos\left[\frac{2\pi}{8760}\left(t - t_\circ - \frac{z}{2}\left(\frac{8760}{\pi\alpha}\right)^{0.5}\right)\right] \quad (10)$$

Errors in equation (10) should not exceed ±1.1°C [21].

The soil, climate, and environment of Nasiriyah are similar to those of Kuwait City. The values are shown in Table 2. [2].

Table 2: Parameters of Kuwait

parameter	Value
Annual amplitude of surface temperature (As)	0.0038 m^2/ h
Thermal diffusivity of soil (α)	13.3 °C m^2/ h
Constant phase (to)	552 h
Mean soil temperature (Tm)	27 ˚C

Therefore, the following formula may be based on equation (10):

$$T_{(z,t)} = 27 - 13.3\, T_{(z,t)} = 27 - 13.3\, e^{-0.31\, z} \times \cos\left[\frac{2\pi}{8760}(t - 552 - 428.31\, z)\right] \quad (11)$$

Numerical solution

Finite-volume techniques are used to numerically solve control equations. The three-dimensional Navier-Stokes equations and three-dimensional continuity equations are solved utilizing computational fluid dynamics (CFD) modeling.

CFD modeling

The EAHE system's performance was modeled by applying CFD to investigate the behavior of the air inside the tube under certain boundary conditions [5]. A basic k-ε model with standard wall treatment was used to forecast turbulence. Heat transmission was represented using the energy equation. The airflow characteristics at numerous system sites were acquired using a dense numerical network. A convergence criterion of 1×10^{-6} was used for both the momentum and energy equations to ensure the efficiency of the numerical result.

Grid independence test

The correctness of the CFD model was assessed using a network independence test. The result remained stable as the number of elements increased, and a network of 2.5 million elements was considered sufficient to achieve numerical stability. Table 3 shows the pipe discharge temperatures and the motor discharge temperatures after cooling.

Table 3: Grid independent check

Element	Outlet motor	Outlet pipe
1803067	308.68637	299.15011
2016828	309.47324	299.26039
2502710	309.7036	299.2604
3005806	309.7035	299.2604

Results and Discussions

Validation

Numerical model accuracy was verified by comparison with a previously published study [3]. The reference study used a 50-meter-long, 0.1016-meter-diameter EAHE system. With an input temperature of 50°C and a tube surface temperature constant equal to the undisturbed soil temperature (26.3°C), the temperature change within the tube was examined at various air velocities (1, 3, 5, 7, and 9) m/s. The current model's solution and those of Hassan et al. [3] match well, as seen in Figure 5, with an average error of approximately 4%. Therefore, the current numerical model can be considered a reliable model for studying the performance of an EAHE.

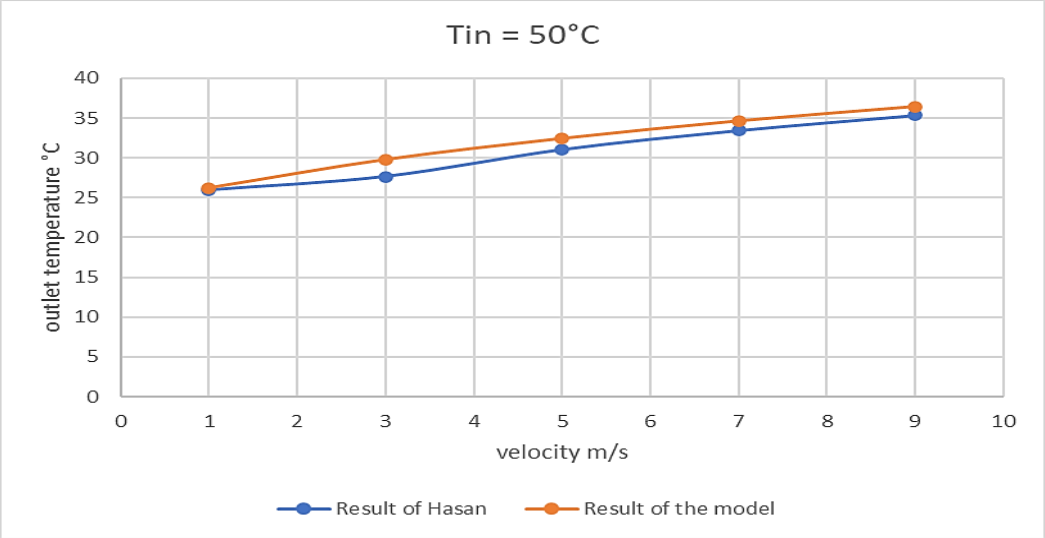

Figure 5: Change in outlet temperature with speed for EAHE compared to the model result.

A.Result

The study was conducted using the FLUENT/ANSYS 2024 software, with the motor designed to its actual dimensions. The study was based on the climatic conditions of Nasiriyah, and results were obtained at inlet air temperatures of 50°C, 40°C, and 30°C. All results shown are calculated based on a 0.6 kg/s mass flow rate.

B.1 Effect of EAHE Pipe Length on External Air Temperature.

Figure 6 illustrates the temperature distribution along a 6-inch-diameter EAHE with a 0.6kg/s mass flow rate. The incoming hot air is at approximately 323 K at the beginning of the tube and then gradually loses heat as it travels through the buried coils due to conduction to the surrounding soil. After several coils, the air temperature drops significantly to about 299 K at the outlet. This temperature fluctuation is steep in the first 15 m of the tube, then turns more moderate. explained by the larger temperature differential between the earth and the air in the first few meters of the tube, which diminishes as the tube length rises.

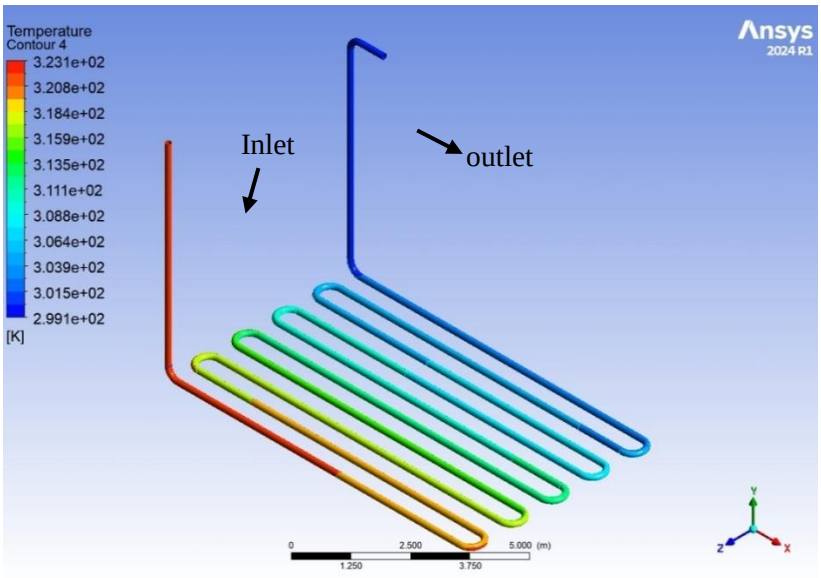

Figure 6: Temperature distribution diagram along the tube of an EAHE at a steady mass flow rate of 0.6 kg/s

Figure 7 illustrates the change in heat output from EAHE with changes in ambient air temperature for all examined tube lengths at a steady 0.6 kg/s mass flow rate. The figure shows that the heat output increases with rising external air temperature due to the increased temperature of the air entering the pipe. The figure also demonstrates that increasing pipe length leads to a greater heat transfer output, resulting from an increased heat transfer surface area and longer contact time between the air inside the tube and the surrounding environment, thus improving heat exchange efficiency.

Figure 8 illustrates the pressure drop for all examined tube lengths at a steady 0.6 kg/s mass flow rate as a function of ambient air temperature. This figure demonstrates that the pressure drop remains steady with rising air temperature since the constant mass flow rate, with the longest length (90 m), exhibits a bigger pressure drop than the other lengths.

Figure 9 illustrates the pumping capacity as a function of ambient air temperature for all examined tube lengths at a steady mass flow rate of 0.6 kg/s. It is noted from this figure that the pressure drop remains steady with rising air temperature, with the longest length (90 m) yielding a higher pumping capacity. This is attributed to the greater pressure drop at a constant mass flow rate.

Figure 10 illustrates the coefficient of performance (COP) with respect to ambient air temperature for all examined tube lengths at a steady 0.6 kg/s mass flow rate. It is noted from this figure that the COP increases with rising air temperature because of increased pumping power and a decrease in the temperature difference. The shorter length (10 meters) yielded a higher COP, while the COP decreases with increasing pipe length.

Figure 11 illustrates the exit temperature from the EAHE tubes for another tube length at all studied temperatures, using a steady mass flow rate of 0.6. It is observed from this figure that the exit temperature reduces with increasing pipe length. This is attributed to the increased heat transfer area and the increased heat retention within the pipe, as the longer the tube, the lower the exit temperature.

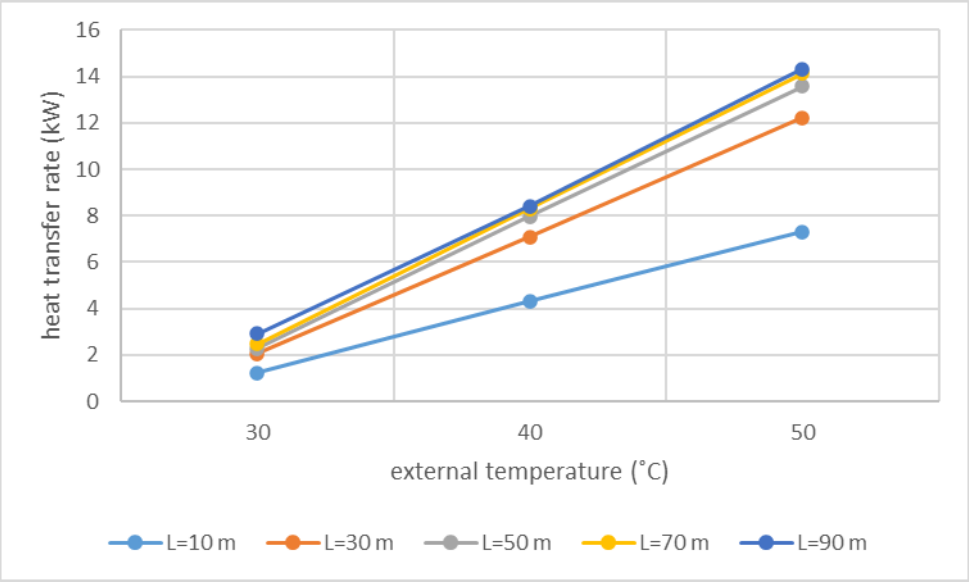

Figure 7: Heat transfer rate variation with external temperature for all examined EAHE tube lengths.

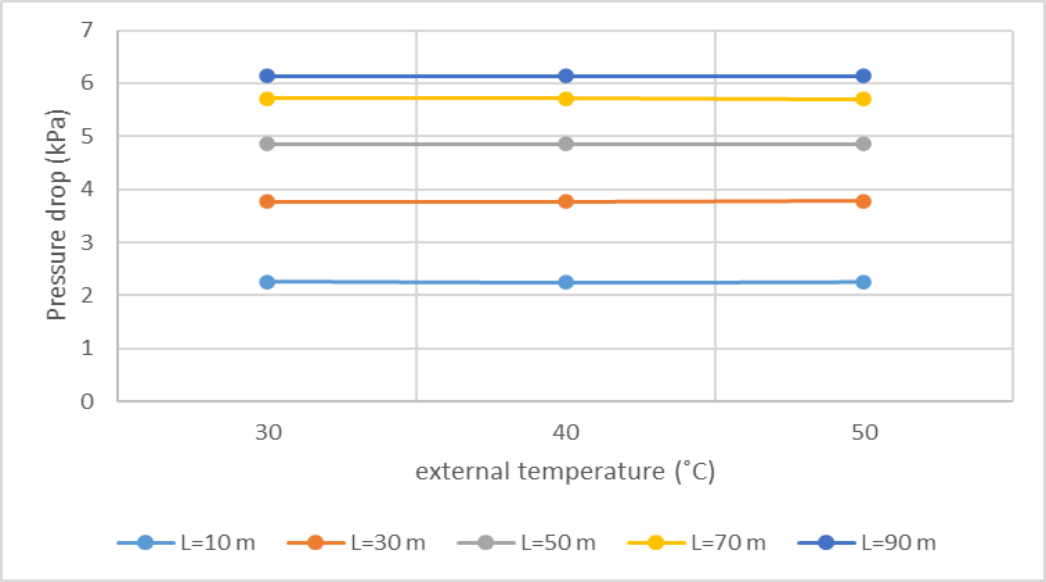

Figure 8: Pressure drop variation with external temperature for all examined EAHE tube lengths.

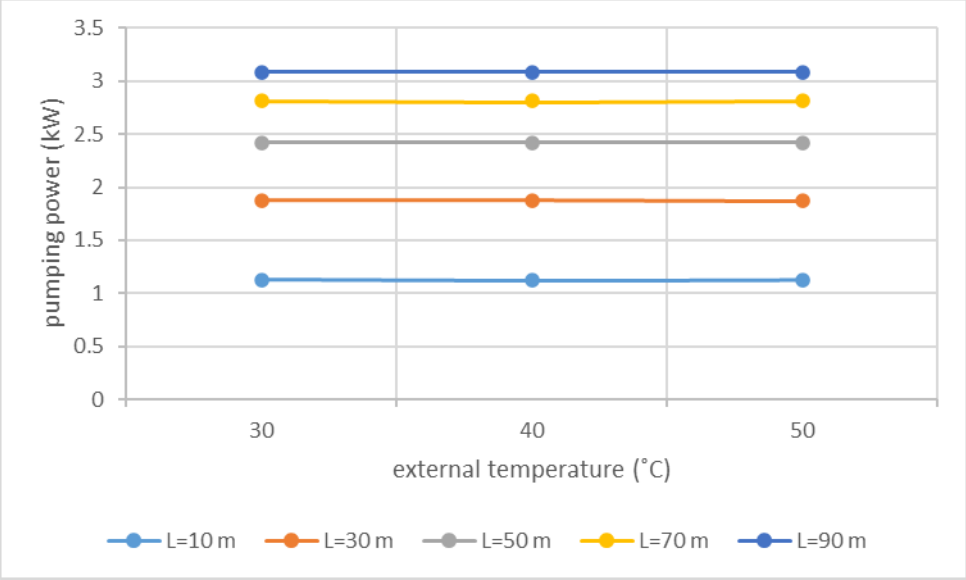

Figure 9: . Pumping power variation with external temperature for all examined EAHE tube lengths.

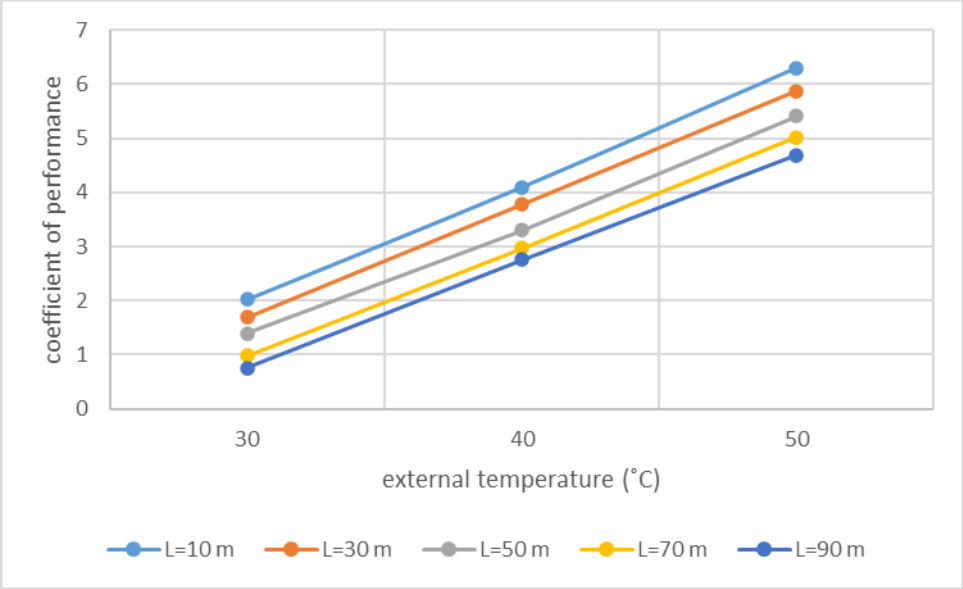

Figure 10: Coefficient of performance variation with external temperature for all examined EAHE tube lengths.

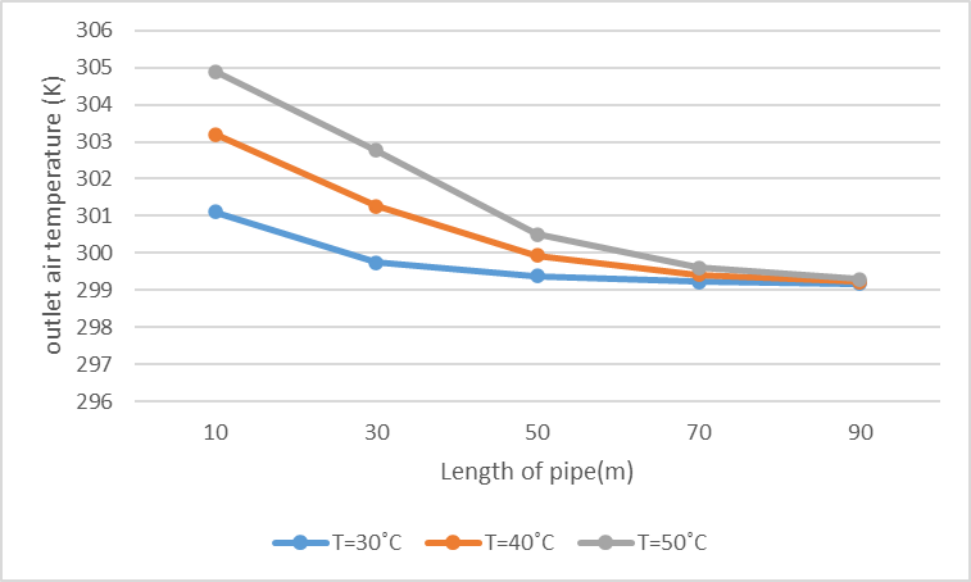

Figure 11: Variation in the temperature of the air exiting the tube with external temperature for all examined EAHE tube lengths.

B.2 The effect of the EAHE system on the temperature of the electric motor

The results indicated an ensuing rise in temperature along the fin surface, which is expected because the air heats up as it moves along the motor surface. Figure 12 shows that the average fin temperature near the air inlet was 299 K (26 °C), as the air heats up as it passes over the fin surface. The highest temperature, 340 K (67°C), is observed towards the left side of the motor casing, away from the air inlet. where the temperature gradually decreases towards the fin tips due to the increased surface area exposed to air and improved heat transfer. This indicates that the cooling system used was effective in improving the thermal performance of the electric motor.

Figures 13, 14, and 15 show the engine temperatures (average, maximum, and minimum) for all studied temperatures at a steady 0,6 kg/s mass flow rate. It is noted from the figure that as the tube length rises, the maximum engine temperature decreases for all inlet temperature values due to the raised surface area and heat transfer time. The greater the pipe length, the lower the temperature compared to other lengths.

Figure 16 illustrates the percentage reduction in engine temperatures for all studied pipe lengths with a diameter of 6 inches. It was observed that the longer the pipe, the greater the percentage reduction, resulting in increased cooling efficiency. The longer pipe (90 m) provided better heat transfer due to the increased air velocity within the system.

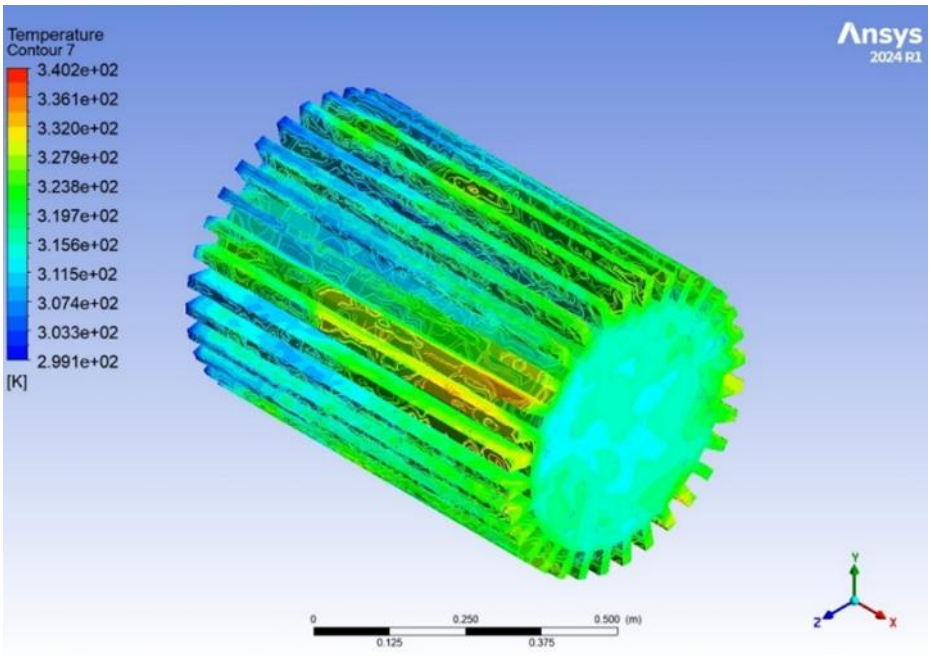

Figure 12: Temperature change along the surface of the fins of the electric motor.

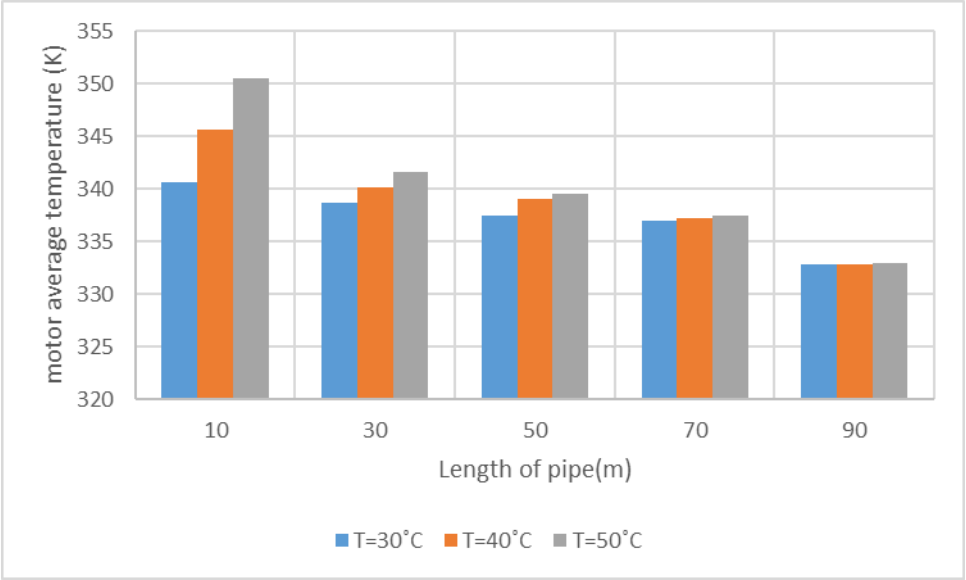

Figure 13: Variation of average electric motor temperature with external temperature for all examined EAHE tube lengths.

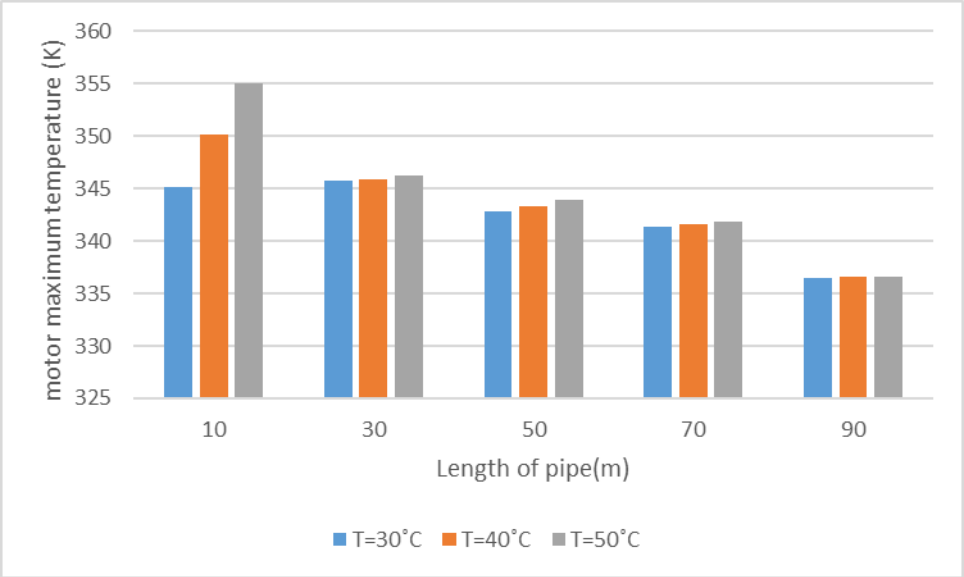

Figure 14: Variation of maximum electric motor temperature with external temperature for all examined EAHE tube lengths.

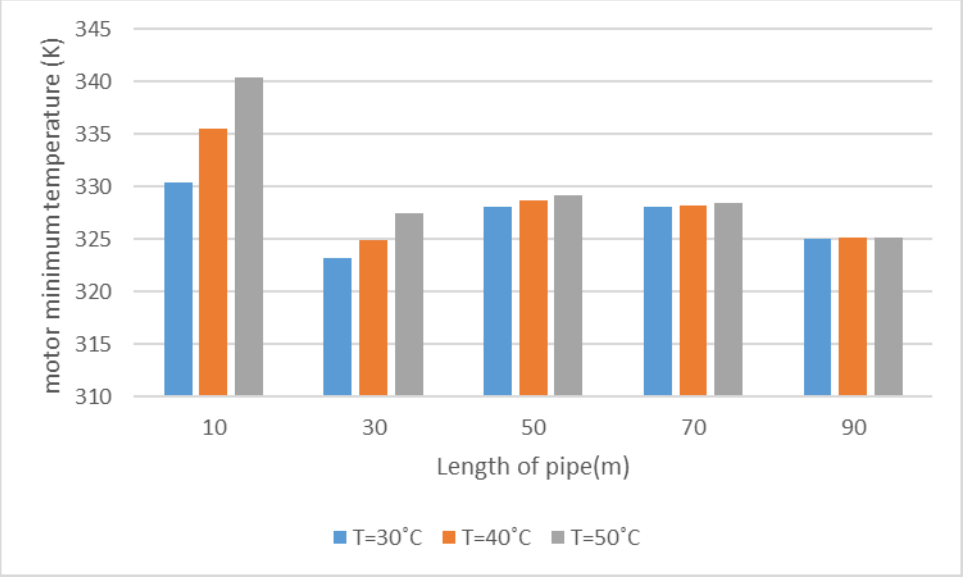

Figure 15: Variation of average electric motor temperature with external temperature for all examined EAHE tube lengths.

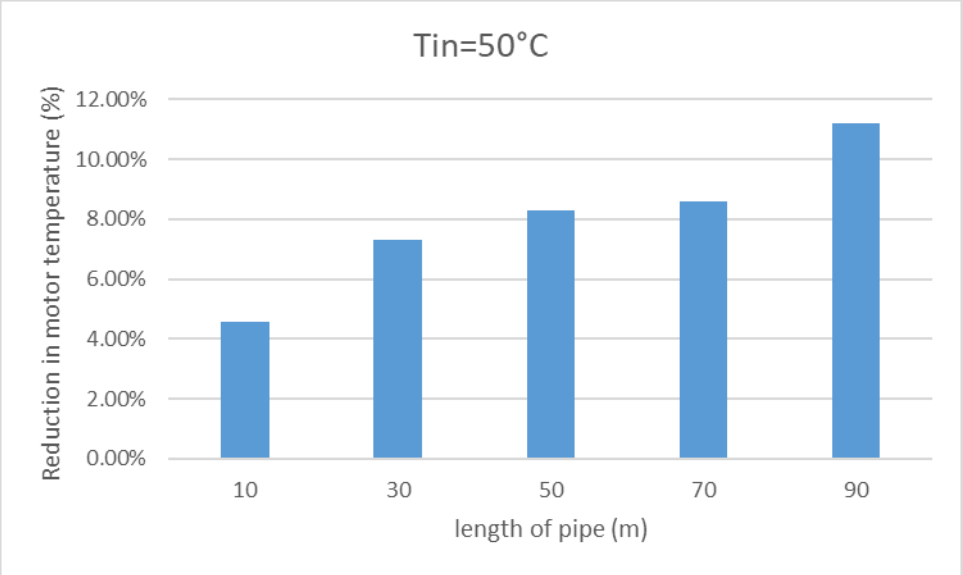

Figure 16: Percentage reduction in engine temperature across all studied pipe lengths with a diameter of 6 in.

Conclusions

This study examines an EAHE design for cooling an electric motor under the climatic circumstances of Nasiri yah city. The impact of length on the efficacy of the EAHE was examined. Upon simulating the examined system and evaluating the outcomes, the subsequent findings were drawn.

1. The reduction in engine temperature was approximately 4.57%, 7.33%, 8.28%, 8.60%, and 11.21% for pipe lengths of 10 m, 30 m, 50 m, 70 m, and 90 m, respectively. This means that the longer the length, the greater the reduction in temperature, resulting in higher system efficiency.
2. As pipe length increases, the pressure drop progressively rises; the longer the pipe, the greater the pressure drop.
3. The electric motor's temperature drops more significantly when the incoming air temperature is higher.
4. As the length of the tube expands, the pressure drop progressively escalates, hence diminishing the coefficient of performance due to the heightened pumping capacity.
5. An efficient passive cooling method for lowering the electric motor's temperature is the earth-air heat exchanger (EAHE), which reduces thermal stress and increases the motor's lifespan.

The suggested EAHE cooling system presents numerous benefits from an industrial standpoint, such as diminished dependence on traditional cooling techniques, decreased energy usage, enhanced

engine dependability, and prolonged service life. This renders the system appropriate for oil pumps functioning in severe heat conditions, such as those seen in factories and power plants.

Nomenclature

C_p	Specific Heat (J/kg K)	Q	heat transfer rate (W)
k	Thermal Conductivity (W/m K)	P.P	pumping power
V	volume flow rate (m^3/s)	ΔP	pressure drop (Pa)
$\dot{m}$	Mass Flow Rate (kg/s)	P.F	Performance Factor
T	Temperature (K)	X	Horizontal Coordinate (m)
P	Total Pressure (Pa)	Y	Vertical Coordinate (m)
L	Length Of Pipe (m)	Z	Axial Coordinate (m)

Greek Symbols

ρ Density (kg/m³)
μ Dynamic Viscosity (m^2/s)

References

[1] M. Benhammou and B. Draoui, "Parametric study on thermal performance of earth-to-air heat exchanger used for cooling of buildings," *Renew. Sustain. Energy Rev.*, vol. 44, pp. 348–355, 2015, doi: 10.1016/j.rser.2014.12.030.

[2] R. M. Hannun, S. H. Hammadi, and M. H. Khalaf, "HEAT TRANSFER ENHANCEMENT FROM POWER TRANSFORMER by," vol. 23, no. 6, pp. 3591–3602, 2019.

[3] M. I. Hasan and A. J. Shkarah, "Parametric study on the performance of the earth - to - air heat exchanger for cooling and heating applications," no. March, 2019, doi: 10.1002/htj.21458.

[4] A. Greco and C. Masselli, "The Optimization of the Thermal Performances of an Earth to Air Heat Exchanger for an Air Conditioning System : A Numerical Study," 2020.

[5] M. I. Hasan and D. M. Muter, "Study the effects configuration and design parameters on the performance of earth to air heat exchanger used in poultry houses," vol. 44, no. 7, pp. 159–179, 2021.

[6] S. N. Ahmad, "Thermal performance evaluation of an earth-to-air heat exchanger for the heating mode applications using an experimental test rig Introduction Energy provides an essential ingredient for all human activities and is also," vol. 43, no. 1, pp. 185–207, 2022, doi: 10.24425/ather.2022.140931.

[7] E. Study, "Archive of SID . ir Archive of SID . ir Archive of SID . ir Archive of SID . ir," vol. 36, no. 01, pp. 78–89, 2023.

[8] C. H. Diedrich, G. Henrique, G. C. Carraro, and V. V. Dimbarre, "Numerical and Experimental Analysis of an Earth – Air Heat Exchanger," 2023.

[9] E. Hummood, M. I. Hasan, and G. Abd, "Investigating the Effects of Disturbed Soil Thickness on the Performance of Earth-Air Heat Exchanger," vol. 42, no. 3, pp. 1101–1110, 2024.

[10] A. R. Nasr, E. A. Badran, and I. I. I. Mansy, "A Novel Cooling Technique to Improve the Thermal Characteristics of a Permanent Magnet Generator Using an Earth – Air Heat Exchanger," vol. 2025, 2025, doi: 10.1155/jece/9987298.

[11] F. Al-Ajmi, D. Loveday, and V.I. Hanby, “The cooling potential of earth-air heat exchangers for domestic buildings in a desert climate”, Building and Environment, Vol. 41, Pp. 235-244, 2006.

[12] N. Sakhri, Y. Menni, A.J. Chamkha, G.L.H. Ameur, N. Kaid and M. Bensaf, “Experimental study of an earth-to-air heat exchanger coupled to the solar chimney for heating and cooling applications in arid regions”, Journal of Thermal Analysis and Calorimetry, Vol. 8, 2020.

[13] M. Rohit, B. Vikas, and A. Abhishek, "Investigation of Thermal Performance of EATHE System under Intermittent Operation: A CFD Approach”, International Journal of Engineering Technology, Management and Applied Sciences, Vol. 4, No. 4, Pp. 2349-4476, 2016.

[14] N. Fuxin, Y. Yuebin, Y. Daihong, and L. Haorong, "Heat and mass transfer performance analysis and cooling capacity prediction of earth to air heat exchanger", Journal of Applied Energy, Vol. 137, Pp. 211–221, 2015.

[15] M. Anuj, K.S. Ankit, and M. Sanjay, "Numerical investigation of the performance and soil temperature recovery of an EATHE system under intermittent operations", Journal of Renewable Energy, Vol. 95, Pp. 510-521, 2016.

[16] C. Pandharpur, D. Ronge, V. Kadam, S. Shende, and P. Kate, “Design of an Earth Air Heat Exchanger System for Space Cooling in Hot and Dry Design of an Earth Air Heat Exchanger System for Space Cooling in Hot and Dry Climate of Pandharpur, India,” no. July 2020.

[17] N. Sakhri, Y. Menni, and H. Ameur, “Effect of the pipe material and burying depth on the thermal efficiency of earth-to-air heat exchangers,” *Case Stud. Chem. Environ. Eng.*, p. 100013, 2020, doi: 10.1016/j.cscee.2020.100013.

[18] Hasan, Mushtaq Ismael. "Influence of wall axial heat conduction on the forced convection heat transfer in rectangular channels." Basrah Journal for Engineering Science 1 (2011): 31-43.

[19] Moreland, F. L., Higgs, F., Shih, J., (editors.), Earth-Covered Buildings Proceeding of Conference in Fort Worth, Texas, USA, May 1978, Washington, DC, D.O.E., 1980. MD, National Bureau of Standards, 1983

[20] Kusuda, Tamami, O. Piet, and John W. Bean, “Annual variation of temperature field and heat transfer under heated ground surfaces, slab-on-grade floor heat loss calculation, Building Science Services, Washington, DC, USA,” 1983.

[21] Labs, K., Cook, J., Passive Cooling, Cambridge, Massachusetts, MIT Press, London, England, 1989